PHYSICAL REVIEW B **81**, 241402(R) (2010)

Magnetoresistance in an aluminum nanoparticle with a single ferromagnetic contact

F. T. Birk and D. Davidović
School of Physics, Georgia Institute of Technology, Atlanta, Georgia 30332, USA

(Received 19 January 2010; revised manuscript received 15 April 2010; published 3 June 2010)

It is found that the magnetoresistance of a nanometer-scale Al particle, attached between a ferromagnetic and an Al lead, has strong asymmetry with respect to the bias voltage. The asymmetric magnetoresistance is explained in terms of the injection of a spin-polarized current from the ferromagnetic lead and the spin accumulation in the particle. The magnetic moment in the particle is parallel to the magnetic field, which is not collinear with the magnetization of the ferromagnetic lead. The field direction changes either discontinuously as the magnetization switches, or continuously as an external magnetic field is being varied, explaining the magnetoresistance.

DOI: 10.1103/PhysRevB.81.241402 PACS number(s): 73.21.La, 72.25.Hg, 72.25.Rb, 73.23.Hk

Spintronics, where controlled manipulation of the spin degree of freedom is pursued,[1,2] offers a rich framework for studying fundamental properties inherent to the physics of nanoscale systems.[3,4] Only a few successful accomplishments on metallic particles coupled to ferromagnetic contacts have been reported.[5–9] In this Rapid Communication we investigate electron transport through a normal-metal particle connected by tunnel junctions to a ferromagnetic lead, *F*, and to an Al lead. This ferromagnet-normal metal-normal metal (FNN) system has been explored in the strong magnetic field regime.[5] In this work we explore magnetoresistance in the regime of low magnetic fields and our main result is the observation of the tunnel-magnetoresistance (TMR) effect.

It is well known that electron transport through a normal metal between two ferromagnetic contacts can exhibit TMR because of the spin accumulation in the normal metal.[10] An interesting point here is that although a single ferromagnetic contact is coupled to the particle, the TMR is still explained in terms of the spin-accumulation mechanism. In carbon nanotubes with a single ferromagnetic contact, TMR has been observed,[11] but not explained. It is now recognized that magneto-Coulomb effects, first studied by Ono *et al.*,[12] can cause magnetoresistance when only one ferromagnetic contact is involved.[5,13]

As discussed later in the text, the TMR observed here, is strongly asymmetric with respect to the bias voltage, which rules out the explanation in terms of the magneto-Coulomb effects. The origin of the TMR is attributed to the electronic magnetic moments occupying the discrete energy levels of the particle, being collinear with the magnetic field in the particle. Therefore, the injection of a spin-polarized current into the particle will result in the accumulation of magnetic moments that are parallel to the magnetic field and not to the magnetization of *F*. The magnetic field inside the particle includes the fringe field generated by *F*, which changes discontinuously as *F* undergoes magnetic transitions. Consequently, the direction of the accumulated magnetic moment will change discontinuously at these transition points, leading to discrete transitions in the TMR. It will be shown later that the direction of the field can be continuously varied by applying a transverse magnetic field, leading to continuous changes in the TMR.

Figure 1 displays a scanning electron microscope image of a representative sample. Out of many tested samples, this particular one has shown the best stability. A larger scale structure is shown in Fig. 1(A), with two needlelike 1-μm-wide leads, overlapping each other near half of the total length. Figure 1(B) shows a higher magnification image of the overlap region, where the tunnel junctions and the particle are confined between the permalloy ($Py=Ni_{0.8}Fe_{0.2}$) and the Al leads. The lower left inset shows the sketch of a shadow mask made of a bilayer resist [methylmethacrylate/polymethyl methacrylate (PMMA)], using electron-beam lithography. The narrowest part in the middle, is just wide enough to be supported and forms a free standing PMMA bridge. In the next step, 200 Å of Py is deposited along direction 1, followed by 15 Å of Al_2O_3, 5 Å of Al, 15 Å of Al_2O_3, and 200 Å of Al, all of them deposited along direction 2. The angles defining directions 1 and 2 are chosen so that the resulting wires barely overlap each other. The inset on the right of Fig. 1(B) shows the cross section of the overlap region with the Al particles embedded in the Al_2O_3 insulating matrix. We use Py as a ferromagnet because it has

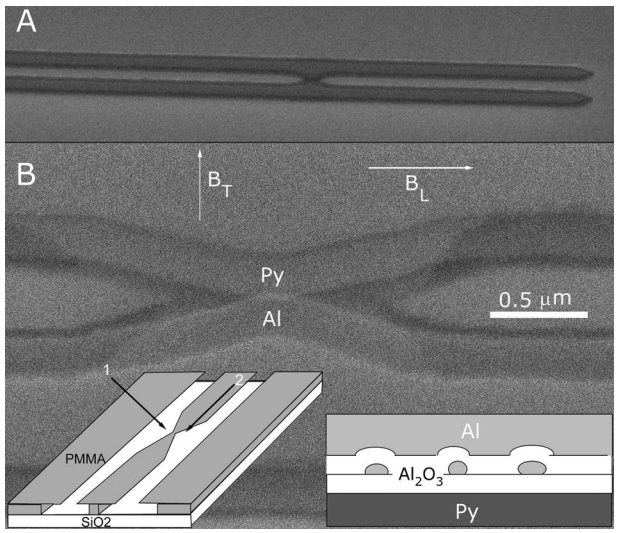

FIG. 1. (A) Large scale SEM image of the device. The leads are 1-μm wide. (B) Close-up image of the junction and magnetic field directions. Lower left inset: sketch of the fabrication process. Lower right inset: sketch of the overlap cross section.

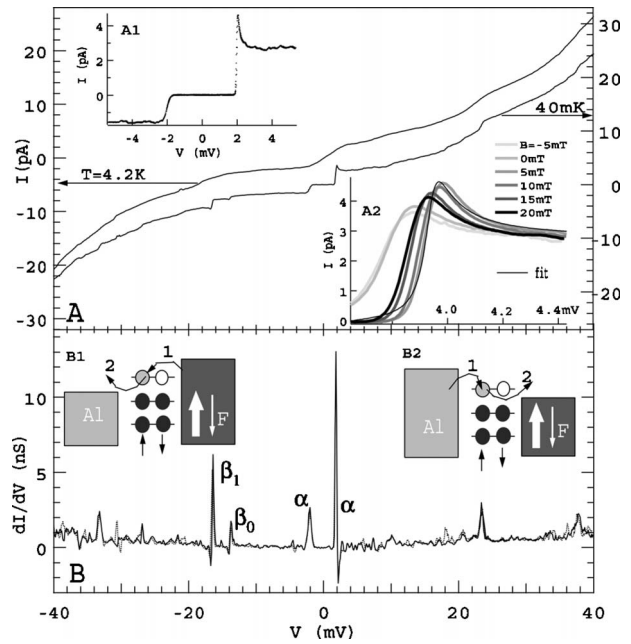

FIG. 2. (A) *I-V* curves in the absence of an applied magnetic field. Inset A1: closeup of the *I-V* curve at $T=40$ mK near the Coulomb-blockade voltage. Inset A2: behavior of the BCS gap for different applied magnetic fields. (B) Conductance versus bias voltage. The energy levels are located at: $V(\alpha)=1.97$ mV and -2.02 mV, $V(\beta_0)=-13.9$ mV, and $V(\beta_1)=-16.5$ mV. Insets B1 and B2: illustration of electron tunneling at negative and positive voltage on F, respectively.

shown a good resistance to oxidation. Imaging by scanning electron microscope[8] determined that the average spacing between Al particles is ~ 10 nm while the particle diameters range is 1–3 nm. The leads were designed with the goal of reaching a single magnetic domain state.

The *I-V* curves at $T=4.2$ K and $T=40$ mK, at zero applied magnetic field, are displayed in Fig. 2(A). Both the Coulomb-blockade (CB) region and the discrete energy levels are well resolved at $T=0.04$ K. The plot of conductance (dI/dV) versus bias voltage is shown in Fig. 2(B), for positive (full line) and negative sweep directions (dotted line).

The sign of the bias voltage is crucial to understand the TMR properties in this report. In Fig. 2(B), the insets B1 and B2 sketch sequential electron tunneling via a discrete energy level of a particle at negative and positive signs of the bias voltage applied on F, respectively. The number of electrons on the particle is even in the CB regime and an electron initially tunnels into the particle. At positive voltage, the first tunneling step takes place when an electron tunnels from the Al lead. In the second tunneling step, an electron is discharged from the particle into F. At negative bias voltage, an electron first tunnels in to the particle from F, followed by an electron tunneling out of the particle into the Al lead. In this discussion we neglected electron spin relaxation in the particle, since the spin-relaxation time, T_1, is in the μsec range,[8,14] which is longer than the electron discharge time into F, $1/\Gamma_F=15$ nsec, as obtained below.

The conductance traces are consistently reproducible along the voltage sweeps. It can clearly be seen that the spacings between discrete energy levels (indicated by conductance peaks), are much larger than the CB-threshold voltage, which is $\approx \pm 2$ mV for this sample, indicating that the background charge, Q_0, is close to $(n+1/2)e$, where n is an integer. Under this condition, only one spin-degenerate level of a single particle is involved in electron transport at low bias voltage. Some of the energy levels display the BCS gap in Al, which arises when the energy of a discrete level of the particle is aligned with the Fermi level in Al.[15] In that case, the level location in the superconducting state is larger than that in the normal state (at $B=0.1$ T), by an amount $(1+C_2/C_1)\Delta/|e|$. Here C_1 and C_2 are the capacitances between the particle and the Py and between the particle and the Al lead, respectively, and Δ is the BCS gap.

By comparing the locations of different levels at positive and negative bias voltage, as well as their shifts when Al is driven normal by the magnetic field, shown in inset A2 in Fig. 2(A), we confirm that the levels α and β have the same capacitance ratio $C_1/C_2=1.2$, while the BCS gap is $\Delta=0.157$ meV. Additionally, we compare the locations of different levels before and after a small Q_0 shift, which confirms the values of C_1/C_2 and Δ. Since the average spacing between Al particles is ~ 10 nm, as discussed earlier, there is more than one particle in the junction shown in Fig. 1. At low voltages, only the particle with a Q_0 closest to $(n+1/2)e$ would conduct; the other particles would remain in the CB regime. Therefore, it should not be surprising that the levels at low bias voltage have equal C_1/C_2 ratios.

In Fig. 2(B), note that at negative bias voltage, the level α, which does not display the BCS gap, is followed by a pair of levels β, which do display the BCS gap; the level α occurs at a voltage where an electron tunnels from the Fermi level of F into the lowest unoccupied level of the particle. It is followed by a pair of levels β, which occur when the closest doubly occupied level, below α, starts to discharge an electron into the Al lead. The discharged electron can leave the particle via distinct excited states. Electron-electron interactions cause splitting of these states, and as a result, multiple conductance levels can be formed out of a single level.[16] The doubling of the second level β, is possible only if the number of electrons on the particle in the CB regime is even. In this case, the excited states generated by the electron discharge process, include both a spin-singlet and a spin-triplet states of the particle. These two states are exchange split, causing the level β to duplicate. For the case of an odd number of electrons in the CB regime, the excited states generated by the electron-discharge process, as described above, would include states from a spin doublet, and β would be a single level.[17]

A spin-up electron discharges at a higher rate because of the larger density of spin-up states in F. As a result, the probability of the spin-up state of the particle being filled is smaller than that for the spin-down state, which is the basic principle behind spin accumulation on the particle. Using elementary techniques outlined in Ref. 18, we find that the current through the particle can be expressed as

$$I = |e| \frac{2\Gamma_{\mathrm{Al}}\Gamma_F(1-P^2)}{2\Gamma_{\mathrm{Al}}+\Gamma_F(1-P^2)}, \tag{1}$$

where Γ_{Al} and Γ_F are the bare tunnel rates between a member of the doublet and the respective leads.

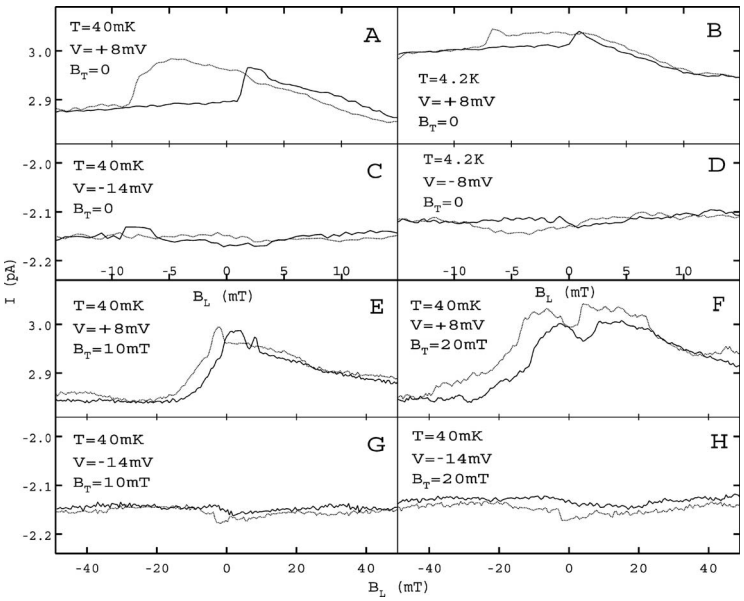

FIG. 3. (A–D) Current versus longitudinal magnetic field at zero transverse magnetic field. (E–H) Similar measurement in the presence of a nonzero transverse magnetic field. Full (dotted) lines correspond to field sweeps in the positive (negative) direction.

At negative voltage on F, inset B1 in Fig. 2, an electron first tunnels into the particle from F. Before tunneling, the particle is in an unpolarized singlet state and therefore, this tunneling process does not depend on P. This time we obtain

$$I = -|e|\frac{2\Gamma_{\mathrm{Al}}\Gamma_F}{\Gamma_{\mathrm{Al}} + 2\Gamma_F}. \tag{2}$$

The tunnel rates can be calculated using Eqs. (1) and (2), and from the current at positive and negative bias voltages in Fig. 2(B). In first approximation, we can neglect the P^2 term because the TMR is weak enough to do so. We find $\Gamma_F = 6.6\times 10^7\ \mathrm{s}^{-1}$ and $\Gamma_{\mathrm{Al}} = 1.1\times 10^7\ \mathrm{s}^{-1}$.

Consider now the TMR measurements shown in Figs. 3(A)–3(D), where graphs of current versus applied longitudinal magnetic field (B_L), at zero applied transverse field ($B_T=0$) are displayed. In order to compare the graphs in Fig. 3, all of the vertical axes were set to equal lengths. At positive bias voltage, Figs. 3(A) and 3(B) show discrete transitions in magnetoresistance at $B\approx -7.5$ mT and $B\approx 2$ mT. At these transitions, the current changes by $\approx 1.5\%$. At negative bias voltage, Figs. 3(C) and 3(D) indicate that the magnetoresistance is suppressed. Figures 3(E) and 3(F) show graphs of current versus B_L for $B_T=10$ mT and $B_T=20$ mT, where B_T is applied perpendicular to the easy axis in the film plane. At negative bias voltage, the TMR remains suppressed, as shown in Figs. 3(G) and 3(H). At positive bias voltage, TMR remains significant with the width of the magnetoresistance signal getting enhanced proportionally to B_T. The asymmetry in the P dependence of the currents given by Eqs. (1) and (2) could explain the asymmetry in the TMR magnitude with bias voltage in Fig. 3. However, there is a caveat. If the magnetic reversal in F is modeled in a standard way, by changing from P to $-P$, the current in Eq. (1) would not change. In order to obtain the TMR, the magnitude of P in Eq. (1) needs to change with the magnetic reversal. As discussed earlier, the electron magnetic moments in the particle are collinear with the magnetic field. The tunnel coupling between the spinors in F, collinear with the magnetization, and the spinors in N, collinear with the magnetic field, depends on ϕ, the angle between these two vectors.[19] The overall effect on the current is that the effective spin polarization to be used in Eq. (1) should be $P\cos(\phi)$ instead of P

$$I = |e|\frac{2\Gamma_{\mathrm{Al}}\Gamma_F[1 - P^2\cos^2(\phi)]}{2\Gamma_{\mathrm{Al}} + \Gamma_F[1 - P^2\cos^2(\phi)]}. \tag{3}$$

If ϕ changes discontinuously at a magnetic transition, then the current given by Eq. (3) will also exhibit a discontinuity, consistent with the transitions in the TMR shown in Figs. 3(A) and 3(B). In addition, as ϕ varies continuously with B_L, a continuous change in current should occur, again in consistency with the TMR background. At negative bias voltage, the current does not depend on P and TMR is thus suppressed, in agreement with our measurements.

It is known that a magnetic transition in F can induce a chemical potential shift in F from the magneto-Coulomb effect related to a magnetoresistance transition.[13] A magneto-Coulomb-based TMR would not exhibit significant asymmetry with bias voltage in our sample. In addition, we have measured TMR at voltages within plateaus of the I-V curves, as in Ref. 8, where the current is nearly constant and a chemical potential shift cannot change the current significantly. Chemical potential shifts due to magneto-Coulomb effect, can be enhanced in ferromagnetic contacts with strong magnetocrystalline anisotropy,[9,20] which is not the case for Py.

For a finite B_T, the TMR remains suppressed at negative bias voltage. A full analysis of the transverse field effect on TMR at positive bias would require the untanglement between changes in the fringe field and changes in the applied magnetic field, but in this case, this information is not available. However, if the applied magnetic field is much larger than the fringe field, then the approximation $\cos^2(\phi) \approx B_L^2/(B_L^2+B_T^2)$ is appropriate. In that case, Eq. (3) predicts that the current through the particle has a *maximum* at $B_L = 0$, in agreement with Figs. 3(E) and 3(F). The presence of

this maximum as well as the suppression of the magnetoresistance at negative bias voltage, indicate that spin accumulation described here is the mechanism underlying the magnetoresistance effect. The width of the magnetoresistance, $2B_T$, is also roughly in agreement with Fig. 3(F). The height of the peak is approximately twice the size of the magnetic transitions in Fig. 3(A). By comparing the peak in Figs. 3(E) and 3(F) with the value predicted by Eq. (3), we can obtain the spin polarization P of the tunnel density of states in Py. Now we can make use of $\cos^2(\phi) \approx B_L^2/(B_L^2+B_T^2)$ at $B_L > 10$ mT, to obtain $P=0.26$, which is consistent with the previously measured value $P \approx 0.28$ in tunnel junctions,[21] but smaller than the $P \approx 0.37$ measured in Py point contacts.[22]

In prior measurements of the FNN quantum-dot system, where F=Co or Ni,[5] the spin polarization was also suppressed (0.08–0.12, in Co), but more so than reported here. It was suggested that tunnel barrier imperfections were responsible for the suppression.[5] Our findings are consistent with that picture. The tunnel barrier in our sample should be less imperfect than that in Ref. 5, because Py is more resistant to oxidation than Co or Ni. A similar suppression of P was observed in ferromagnetic tunnel junctions based on pure Ni leads, relative to P in ferromagnetic tunnel junctions based on Ni-Fe alloys as leads.[21] In that case, the reduction in P in the Ni lead was attributed to the sensitivity of the Ni surface.

In order to obtain a better understanding about the fringe field, we can study its pair-breaking effect on the BCS gap. In Fig. 2(A), inset A2, we measure the BCS gap as a function of the applied magnetic field B_L. There was a small Q_0 shift between Fig. 2, inset A2, and the rest of the figures, which caused level α to shift from 1.97 to 3.89 mV. At the applied fields of −5 mT and 0 T, I versus V is measured before the magnetic transition at 2 mT, while at $B_L \geq 5$ mT, I versus V is measured after the transition. The BCS gap has a clear discontinuity at the transition, indicating a discontinuity in the fringe field. Analogous behavior was observed around the magnetic transition in the reversed direction of the field sweep.

The fringe field at $B_L \geq 5$ mT, is weak because the BCS gap is relatively large. We fit the current versus voltage data to the broadened BCS density of states: $I = I_0 \mathrm{Re}\frac{V-V_0}{\{(V-V_0)^2-[(\Delta-i\gamma)(C_1+C_2)/C_1]^2\}^{1/2}}$, and the best fitting is shown at $B_L=5$ mT, with a corresponding BCS gap $\Delta = 0.155 \pm 0.007$ meV and broadening $\gamma = 21 \pm 0.7$ μeV. We fit the entire family of curves in Fig. 2(A), inset A2, well to this formula, using the same parameters I_0 and V_0, the level current and location, respectively, while Δ and γ are varied with B_L. For $B_L \geq 5$ mT, we find the BCS gap is reduced at a rate $d\Delta/dB_L = -2.29$ meV/T. Our BCS gap is close to $\Delta_0 = 0.172$ meV, the BCS gap measured in Al particles with all Al leads, in zero magnetic field.[15] In our case, the magnetic field, at $B_L=5$ mT, is estimated as $(\Delta_0-\Delta)/|d\Delta/dB| = 9$ mT. So the fringe field is ~mT, justifying the approximation for $\cos^2(\phi)$.

In conclusion, we demonstrated a spin-accumulation mechanism of magnetoresistance in a normal-metal particle with a single ferromagnetic contact. If the magnetic field on the particle is not parallel to the magnetization, the injection of a spin-polarized current into the particle will result in the accumulation of the magnetic moment not being parallel to the magnetization of the ferromagnetic lead. The angle between the accumulated magnetic moment and the magnetization changes with the applied magnetic field, causing magnetoresistance. This simple mechanism needs to be considered when interpreting results in spintronics involving discrete energy levels.

This research is supported by the DOE under Grant No. DE-FG02–06ER46281.

[1] S. A. Wolf, D. D. Awschalom, R. A. Buhrman, J. M. Daughton, S. von Molnar, M. L. Roukes, A. Y. Chtchelkanova, and D. M. Treger, Science **294**, 1488 (2001).
[2] I. Žutić, J. Fabian, and S. D. Sarma, Rev. Mod. Phys. **76**, 323 (2004).
[3] P. Seneor, A. Bernand-Mantel, and F. Petroff, J. Phys.: Condens. Matter **19**, 165222 (2007).
[4] J. Barnaś and I. Weymann, J. Phys.: Condens. Matter **20**, 423202 (2008).
[5] M. M. Deshmukh and D. C. Ralph, Phys. Rev. Lett. **89**, 266803 (2002).
[6] A. Bernand-Mantel *et al.*, Appl. Phys. Lett. **89**, 062502 (2006).
[7] K. Yakushiji, S. Mitani, K. Takanashi, S. Takahashi, S. Maekawa, H. Imamura, and H. Fujimori, Appl. Phys. Lett. **78**, 515 (2001).
[8] Y. G. Wei, C. E. Malec, and D. Davidovic, Phys. Rev. B **76**, 195327 (2007).
[9] A. Bernand-Mantel, P. Seneor, K. Bouzehouane, S. Fusil, C. Deranlot, F. Petroff, and A. Fert, Nat. Phys. **5**, 920 (2009).
[10] M. Johnson and R. H. Silsbee, Phys. Rev. Lett. **55**, 1790 (1985).
[11] A. Jensen, J. R. Hauptmann, J. Nygard, and P. E. Lindelof, Phys. Rev. B **72**, 035419 (2005).
[12] K. Ono, H. Shimada, and Y. Outuka, J. Phys. Soc. Jpn. **66**, 1261 (1997).
[13] S. J. van der Molen, N. Tombros, and B. J. van Wees, Phys. Rev. B **73**, 220406(R) (2006).
[14] Y. G. Wei, C. E. Malec, and D. Davidovic, Phys. Rev. B **78**, 035435 (2008).
[15] D. C. Ralph, C. T. Black, and M. Tinkham, Phys. Rev. Lett. **74**, 3241 (1995).
[16] O. Agam, N. S. Wingreen, B. L. Altshuler, D. C. Ralph, and M. Tinkham, Phys. Rev. Lett. **78**, 1956 (1997).
[17] We confirm the relation between parity and multiplicity by measuring the Zeeman splitting of the levels.
[18] E. Bonet, M. M. Deshmukh, and D. C. Ralph, Phys. Rev. B **65**, 045317 (2002).
[19] F. T. Birk, C. E. Malec, and D. Davidovic, Phys. Rev. B **79**, 245425 (2009).
[20] B. G. Park, J. Wunderlich, D. A. Williams, S. J. Joo, K. Y. Jung, K. H. Shin, K. Olejnik, A. B. Shick, and T. Jungwirth, Phys. Rev. Lett. **100**, 087204 (2008).
[21] R. Meservey and P. M. Tedrow, Phys. Rep. **238**, 173 (1994).
[22] R. J. Soulen *et al.*, Science **282**, 85 (1998).